Construction and Building Materials xxx (xxxx) xxx

Contents lists available at ScienceDirect

Construction and Building Materials

journal homepage: www.elsevier.com/locate/conbuildmat

On-site measurement of heat of hydration of delivered mass concrete

Hung-Liang (Roger) Chen *, Seyednavid Mardmomen, Guadalupe Leon

Dept. of Civil and Environmental Engineering, West Virginia University, P.O. Box 6103, Morgantown, WV 26506-6103, USA

HIGHLIGHTS

- A 1-m concrete cube was developed to obtain ATR using cube's center temperature.
- Required cube insulation was provided for ambient conditions between −10 °C to 30 °C.
- Heat of hydration measurements were demonstrated during four on-site castings in WV.
- Hydration heat from concrete containing slag or fly ash replacement was obtained.
- ATRs from on-site cube compared well with adiabatic and isothermal calorimetry data.
- Heat generation functions were accurately obtained using the ATRs measured on-site.

ARTICLE INFO

Article history:
Received 15 July 2020
Received in revised form 27 September 2020
Accepted 5 October 2020
Available online xxxx

Keywords:
Mass concrete
Semi-adiabatic calorimetry
Heat of hydration
Adiabatic temperature rise
Degree of hydration
Specific heat
Heat generation function
Isothermal calorimetry
Fly ash
Slag

ABSTRACT

In this study, measurements of the heat of hydration of mass concrete delivered on-site were proposed. A one-meter concrete cube, cast adjacent to the real structure, was developed as an on-site semi-adiabatic calorimeter. A table was established for the required insulation of the cube in different ambient temperatures. To simplify the measurement process and cost, a method was developed to obtain the concrete adiabatic temperature rise (ATR) by simply using the measured temperature at the center of the cube. The finite element method (FEM) was used to calculate the required insulation for various ambient conditions between −10 to 30 °C so that the ATR could be accurately estimated using only the measured center temperature. The predicted ATR and the actual ATR showed less than 1% error. The proposed heat of hydration measurement was tested during four on-site field castings at three different districts in West Virginia. Two of the field batches contained 50% Grade 100 ground granulated blast furnace slag replacements. The fourth field batch had 30% Class F fly ash replacement. The material collected from each field test was also used to perform laboratory adiabatic and isothermal heat of hydration measurements. The ATR calculated from the on-site cube data compared well with the results from both adiabatic and isothermal calorimetry tests. The heat of hydration parameters were successfully obtained based on the ATR calculated from each on-site casting. Results show that the proposed on-site heat measurement can be a simple and accurate approach to measure the heat of hydration of a delivered concrete batch.

1. Introduction

The curing process of concrete is an exothermic chemical reaction between the cementitious material and the mixing water. The adiabatic temperature rise (ATR) can be significant, depending on the mix proportions and cementitious chemical compositions. High ATRs increase the possibility of thermal cracking in mass concrete structures since the surface of the concrete tends to cool down much faster than the inside layers. A precise estimation of the ATR is vital to model the thermal and mechanical behavior of concrete at an early age. Several test methods are available to determine the heat of hydration of concrete. Isothermal, semi-adiabatic, and adiabatic calorimetry are the standard test methods that have been used by many researchers [1–10]. De Shutter et al. [1] measured the evolution of the heat of hydration of concrete using isothermal calorimetry with curing temperatures of 5, 20, and 35 °C and adiabatic calorimetry. Broda et al. [2] designed an isothermal calorimeter to measure the heat of hydration of cylindrical samples in different curing temperatures (10, 20, 30, and 40 °C). Gibbon et al. [9] designed a low-cost adiabatic calorimeter that was controlled using a computer system. Lin and Chen [10] developed an adiabatic calorimetry modifying Gibbon et al.'s design to control the curing water temperature to match the concrete temperature. Instead of reaching the exact adiabatic condi-

* Corresponding author.
E-mail addresses: roger.chen@mail.wvu.edu (Hung-Liang (Roger) Chen), semardmomen@mix.wvu.edu (S. Mardmomen), gleon@mix.wvu.edu (G. Leon).

https://doi.org/10.1016/j.conbuildmat.2020.121246
0950-0618/

tion, a semi-adiabatic calorimeter may provide a more practical way to measure the heat of hydration because it requires a less complicated controlling unit [11–18].

For a semi-adiabatic calorimeter, the heat loss due to the ambient conditions needs to be estimated and added back to calculate the ATR. RILEM TC 119-TCE [18] introduced a semi adiabatic calorimeter made of an insulated vessel filled with foam rubber and an external shell. Based on this document, the calorimeter's coefficient of heat loss shall not exceed 100 J/hr/K in a fixed ambient temperature of 20 °C. Zhang et al. [11] used a cylindrical container to evaluate the effect of the water-cement ratio, superplasticizer, and mineral admixtures on the hydration heat. Schindler et al. [12] used an insulated steel drum with a cylindrical concrete specimen to quantify the hydration development of different concrete mixes containing various amounts of slag and fly ash. Eddhahak et al. [16] used a Langavant type semi-adiabatic test to measure the heat generated by fresh PCM-mortars specimens. Klemczak et al. [17] used isothermal and semi-adiabatic calorimetry to test several mixes with cement, limestone, slag, and siliceous fly ash. Ng et al. [14,15] compared a 25-cm cubic adiabatic calorimeter versus two 50-cm and 1-m cube as semi-adiabatic curing test setups. Heat loss characteristic coefficients were calculated using four temperature measurements in the cubes to calculate the ATR. Riding et al. [13] used semi-adiabatic calorimetry devices at several construction sites under controlled ambient temperature.

Besides laboratory measurement of the heat of hydration, on-site measurements of the temperature of concrete have been conducted [10,19–21]. Tia et al. [19] used a 1-m cube to measure the temperature of delivered concrete on-site to validate the correctness of hydration parameters in a finite element analysis. Do [20] monitored the temperature development of three different bridge pier footings cast in Florida. Lin and Chen [10] monitored two 1.2-m concrete cubes with steel formwork and embedded temperature sensors to validate their hydration model in a finite element model. Yikici and Chen [21] constructed four 2-m concrete cubes in various locations throughout West Virginia with concrete containing slag, and Class F fly ash.

In this study, measurements of the heat of hydration of mass concrete delivered on-site were proposed. A one-meter concrete cube, cast adjacent to the real structure, was chosen as an on-site semi-adiabatic calorimeter. A table was developed for the required insulation for the cube in different ambient temperatures. To simplify the measurement process and cost, a method was developed to obtain the concrete ATR simply by using the measured temperature at the center of the cube. The proposed heat of hydration measurement was tested during on-site castings at three different districts in West Virginia.

2. Design

A one-meter (1-m) cube with multiple layers of insulation (shown in Fig. 1) was built in a way that minimizes the amount of heat loss to the ambient environment. Plywood was used to create the structure of the cube, and polystyrene foam boards were cut into pieces and placed on each side of the cube. The 1-m cube specimen was chosen to act as semi-adiabatic calorimetry. A temperature logger was embedded to measure the temperature–time history at the center of the cube and another logger was used to measure the ambient temperature. The temperature–time history of the cube's center was used to calculate the ATR of the delivered concrete batch. The amount of insulation for different ambient conditions can be adjusted based on a heat loss analysis to ensure the accuracy of the measured ATR.

3. Analysis

The governing equation for a 3D heat transfer problem can be expressed as:

$$\frac{k}{\rho C_p}\left(\frac{\partial^2 T}{\partial x^2}+\frac{\partial^2 T}{\partial y^2}+\frac{\partial^2 T}{\partial z^2}\right)+\frac{q(t)}{\rho C_p}=\frac{\partial T}{\partial t} \tag{1}$$

where T is the temperature (°C), x, y and z are the coordinates, t is time, k is the thermal conductivity (W/m/K), C_p is the specific heat (J/kg/°C) and $q(t)$ is the heat generation function of the volume (W/m^3). For a concrete specimen subjected to a semi-adiabatic condition, the following equation can be expressed between the adiabatic temperature rise and the amount of heat loss:

$$T_{Vol}-T_{ini}=T_{ad}-\frac{H_{Loss}}{\rho C_p} \tag{2}$$

where, $T_{Vol}, T_{ini}, T_{ad}, H_{Loss}$, ρ, and C_p are measured volumetric mean temperature, initial temperature, adiabatic temperature rise, the amount of heat loss, density, and specific heat of concrete.

According to the heat conduction law (Fourier's Law), the rate of the heat loss vs. time $\partial H_{Loss}/\partial t$ between the specimen and the

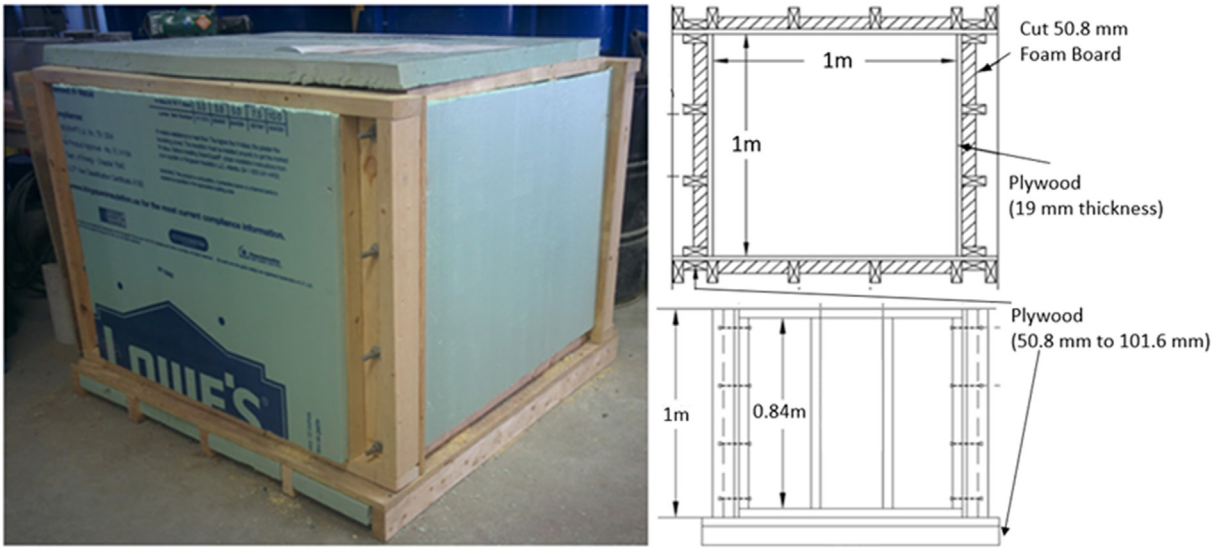

Fig. 1. 1-m cube setup.

ambient environment is proportional to the average thermal conductivity of the system multiplied by the temperature difference between the surface of the concrete and ambient temperature. The heat loss is dependent upon the surroundings, including the formwork, insulation foam, or blanket which all have different thermal resistance. The overall heat loss can be determined using the following relationship [14]:

$$H_{Loss} = \int_0^t \lambda \rho C_p (T_{Surf} - T_{Amb}) dt \tag{3}$$

where T_{Surf} and T_{Amb} are the surface mean temperature of the concrete and the ambient temperature and λ represents the heat loss characteristic coefficient of the system. By substituting Eq. (3) into Eq. (2), the adiabatic temperature rise of the concrete can be calculated with the following equation:

$$T_{ad} = T_{Vol} - T_{ini} + \int_0^t \lambda (T_{Surf} - T_{Amb}) dt \tag{4}$$

By taking a derivative of Eq. (4), the following expression will be obtained:

$$\frac{\partial T_{ad}}{\partial t} = \frac{\partial T_{Vol}}{\partial t} + \lambda (T_{Surf} - T_{Amb}) = \frac{q(t)}{\rho C_p} \tag{5}$$

The spatial temperature profile, $T(x,y,z)$, within the concrete volume, is no longer location-dependent when enough insulation is provided. Hence, the calculation process can be greatly simplified where T_{Vol} and T_{Surf} can be assumed to be equal to the measured center temperature, T_c. Therefore,

$$\frac{\partial T_c}{\partial t} + \lambda (T_c - T_{Amb}) = \frac{q(t)}{\rho C_p}$$

$$T_c(t) = \exp(-\lambda t)\left(\int_0^t \exp(\lambda t)\left(\frac{q(t)}{\rho C_p} + \lambda T_{Amb}\right) dt + T_{ini}\right) \tag{6}$$

It was observed that after a long period of time, the concrete, which was cured under high temperature from its own heat of hydration, would mature faster, and the production of the hydration heat would reach a plateau. Therefore, ∂T_{ad} will be approximately equal to zero (constant adiabatic temperature). Ng et al. [15] proposed 120 h after the concrete placement to be enough time to reach the constant adiabatic temperature based on several experiments. In this study, it was assumed that the heat generation was negligible after 140 h instead since mixes with slag and fly ash can still produce heat even after 120 h. Therefore, an average heat loss characteristic coefficient can then be obtained after 140 h using the following equation:

$$\lambda_1 = -\frac{\frac{\partial T_c}{\partial t}}{(T_c - T_{Amb})} \tag{7}$$

3.1. Heat loss characteristic coefficient

To assume that T_{Vol} and T_{Surf} are equal to the temperature measured at the center location of the cube, a minimum amount of insulation needs to be calculated. The minimum amount depends on the different ambient environmental conditions. A finite element method (FEM) using a user subroutine [10] in ABAQUS program was developed to find the minimum insulation needed. A 1-m cube of concrete surrounded by 1.9-cm thickness of plywood formwork and 2.54-cm thickness of insulation was modeled in the FEM program. Perfect bond (tie constraints) were used between the plywood, insulation material, and concrete. Hexahedral linear element (DC3D8) with a size of 1.9-cm was found to be enough for convergence. The mass densities of the concrete, plywood, and insulation foam were 2286.6, 672.8, and 30.4 (kg/m^3), respectively. The specific heat of 1256 and 2261 (J/kg/°C) were used for the insulation foam board and plywood materials, respectively. The thermal conductivity of the plywood was assumed to be 0.13 W/m/K. The specific heat (C_p) and thermal conductivity (K_c) of the concrete were considered to be degree of hydration dependent [13,22]. They were calculated in a user subroutine with Eq. (8) and Eq. (9). A weighted average (using the proportions of cement, slag and fly ash in each mix) specific heat of cementitious materials (C_{cem}) can be assumed to calculate the ATR from the heat of hydration when the mixes contained slag or fly ash. Krishnaiah et al [23] measured the specific heat of supplementary cementitious materials at different compaction levels. The values of 640 and 720 J/kg/°C were reported for slag and fly ash, respectively.

$$C_p(\alpha_r, T(t)) = \frac{1}{\rho}(W_{cem}\alpha_r(8.4T(t) + 339) + C_{cem}W_{cem}(1 - \alpha_r) + 710W_s + 840W_a + 4184W_w)$$

$$C_{cem} = 740P_{cem} + 640P_{SL} + 720P_{FA} \tag{8}$$

$$K_c(\alpha_r) = K_{uc}(1.33 - 0.33(\alpha_r(t)) \tag{9}$$

where $\alpha_r = \alpha/\alpha_u$, α is the degree of hydration of the concrete, α_u is the ultimate degree of hydration, ρ is the mass density of concrete, W_{cem}, W_s, W_a and W_w are the mass of cementitious materials, sand, coarse aggregate and water per unit volume of concrete (kg/m^3), T(t) is the temperature of concrete (°C), and K_{uc} is the thermal conductivity (W/m/K) of the mature concrete (measured after 28 days of curing). P_{cem}, P_{SL}, and P_{FA} are the mass fractions of cement, slag, and fly ash, respectively, in the cementitious materials.

In the FEM subroutine, the heat release, $H(t_e)$, was assumed to be an exponential function with two empirical hydration parameters (τ and β) shown in Eq. (10). The degree of hydration can be obtained using the heat release of concrete divided by the ultimate heat of hydration (H_u) and mass of cementitious materials in a unit volume of concrete (W_{cem}). The ultimate heat of hydration is a quantity dependent on the chemical properties of the cementitious materials. Since the temperature of the concrete can affect the chemical reaction between the cementitious materials and water, the time shift was considered with the Arrhenius law of chemical reaction using the equivalent age (t_e) concept in Eq. (11). In the Arrhenius equation, the reference temperature was assumed to be 23 °C and the time step was set to be 0.2 h to reach convergence in the numerical integrations. Therefore, the heat generation function, $q(t)$ of each concrete element can be calculated using the following equations:

$$H(t_e) = H_u W_{cem}\alpha_u \exp\left(-\left[\frac{\tau}{t_e}\right]^\beta\right), \ \alpha(t_e) = \frac{H(t_e)}{H_u W_{cem}} \tag{10}$$

$$t_e = \int_0^t \exp\left(-\frac{E_a}{R^*}\left(\frac{1}{T(t)+273} - \frac{1}{23+273}\right)\right) dt \tag{11}$$

$$q(t) = H_u W_{cem}\alpha_u exp\left(-\left[\frac{\tau}{t_e}\right]^\beta\right)\left[\frac{\tau}{t_e}\right]^\beta \times \frac{\beta}{t_e} exp\left(-\frac{E_a}{R^*}\left(\frac{1}{T(t)+273} - \frac{1}{23+273}\right)\right) \tag{12}$$

where τ,β are the hydration parameters, t is the time, T is the temperature of concrete (°C), R^* is the universal gas constant (8.314 J/mol/K) and E_a is the activation energy of concrete. In the FEM analyses, the initial temperature of the concrete was assumed to be 30 °C. The parameters used in the FEM model are shown in Table 1. The ultimate thermal conductivity of concrete was measured following the CRD-C standard for the concrete [10,24]. The activation energy for the mix was measured [25] following ASTM

Table 1
Input parameters for FEM thermal analysis.

H_u (J/g)	α_u	E_a (J/mol)	τ	β	K_{uc} (W/m/K)	W_{cem}(Kg/m^3)	W_s(Kg/m^3)	W_a(Kg/m^3)	W_w(Kg/m^3)
498,970	0.703	41,841	14	0.94	1.765	334.6	843.63	969.11	139.41

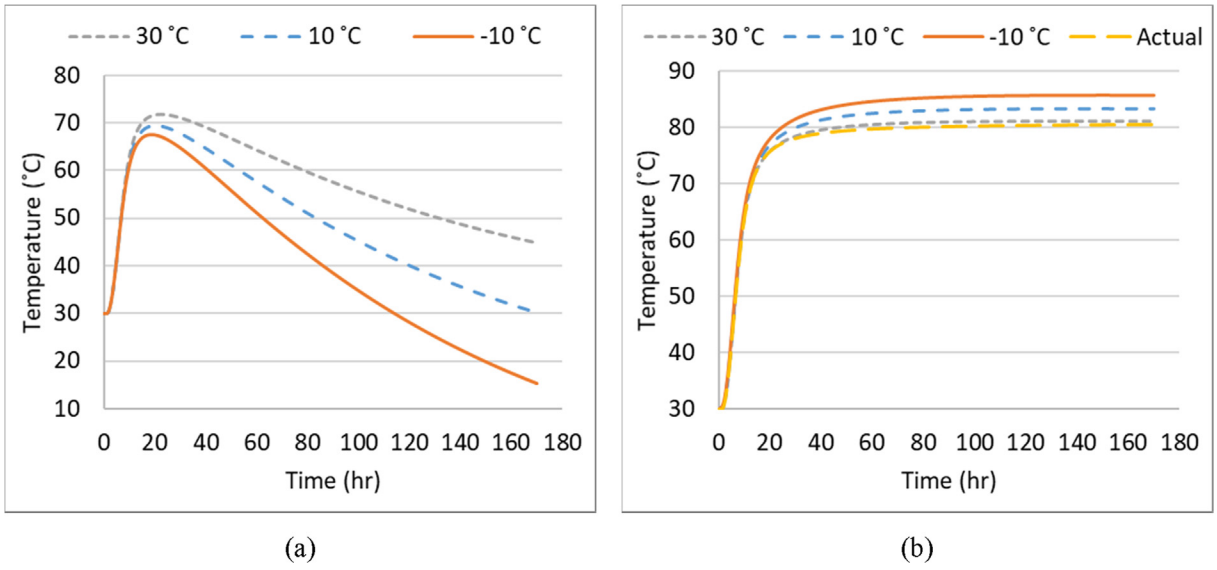

Fig. 2. The effect of ambient temperature on the temperature at the center location (a) Center temperatures and (b) Calculated ATRs versus the actual ATR.

Table 2
Required insulation for different ambient temperature.

T_{Amb}(°C)	Thermal Conductivity of insulation (W/m/K)	RSI value of insulation (m^{2}K/W) (Each Layer = 0.88 m^{2}K/W)	$T_{c,max}$ (°C)	λ_1 (hr^{-1})	$\lambda_1(T_{c,max} - T_{Amb})$
−10	0.01038	2.448 (2.78 Layers, R = 13.89)	70.63	0.00345	0.2784
0	0.01124	2.259 (2.57 Layers, R = 12.82)	70.99	0.00369	0.2617
10	0.01297	1.958 (2.23 Layers, R = 11.11)	71.30	0.00415	0.2547
20	0.01557	1.632 (1.85 Layers, R = 9.26)	71.68	0.00482	0.2491
30	0.02075	1.224 (1.39 Layers, R = 6.94)	72.11	0.00605	0.2548

C-1074. A convection film coefficient of 7.9 W/m^2/K (free convection) was assumed for the surface convection heat transfer between the ambient air and the surface of the insulation materials. The thermal conductivity of the foam was assumed to be 0.0289 (W/m/K) or RSI value of 0.88 (m^2 K/W) for the 25.4-mm insulation foam board which is equivalent to an R-value of 5.

Fig. 2(a) shows the change in the center temperature due to the variation of a constant 7-day ambient temperature from −10 °C to 30 °C. It is evident that by lowering the ambient temperature, the cube loses more heat to the environment. Eq. (7) and Eq. (13) were used to calculate ATR, Fig. 2(b), using the center temperatures from Fig. 2(a). As shown in Fig. 2(b), the calculated ATR using λ_1 from Eq. (7) would be overestimated for both the −10 °C and 10 °C ambient cases due to insufficient insulation, and the insulation was barely enough for the 30 °C case.

Using the FEM program, the amount of insulation was estimated so that the calculated ATR using the one-point measurement could be close to the actual ATR of the mix. The thermal conductivity of the 25.4-mm insulation was modified until the calculated heat losses were minimized and the calculated ATR using the center temperature approached the actual ATR. The amount of insulation needed for each ambient temperature is shown in Table 2. The required number of minimum insulation layers using the 25.4-mm thickness foam board with an RSI value of 0.88 (m^2.K/W) are shown together with their minimum R values of insulation corresponding to each ambient condition. The heat loss characteristic coefficient (λ) versus time for each ambient case calculated using Eq. (4) with the actual ATR (as T_{ad}) and center temperatures (as both T_{Vol} and T_{Surf}), is shown in Fig. 3. It can be seen that λ approached constant values after 140 h in all the cases which is a validation for the usage of a constant λ_1 obtained after 140 h.

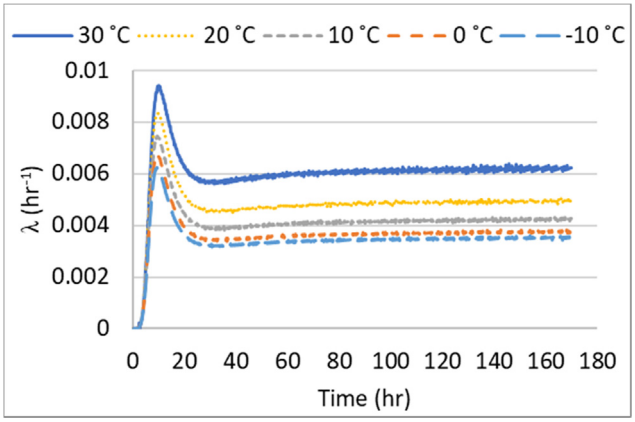

Fig. 3. Heat loss characteristic comparisons vs. time.

The amount of insulation needed for each ambient temperature and the heat loss coefficient, λ_1 are also shown in Table 2. As shown in Table 2, the heat loss amount, expressed as λ_1 times the maximum center temperature ($T_{c,max}$) minus the average ambient temperature (T_{Amb}), remained in a constant range. This heat loss upper bound limitation is about 0.25. When $\lambda_1(T_{c,max} - T_{Amb})$ has a value higher than 0.25, the concrete cube has too much heat loss and the heat compensation method would not be applicable. However, when the insulation requirements under each ambient condition shown in Table 2 are met, the ATR can be accurately obtained. The cube's center temperatures, T_c under different ambient conditions (with the corresponding insulation from Table 2) are shown in Fig. 4(a). The ATR curves calculated using Eq. (13) are plotted on Fig. 4(b) for the cubes under different ambient temperatures, and the results show that the ATR agrees very closely with the actual ATR with less than 1.0% error for each ambient condition (from −10 °C to 30 °C) when sufficient insulation is provided.

It was found that a daily ambient temperature variation up to 30 °C has little effect on the center temperature using FEM analysis. A sinusoidal ambient temperature varying between −25 °C to 5 °C with a daily average of −10 °C was applied with the insulation (RSI = 2.448), and results show that the peak temperature at the center of the cube would only have about 0.5% difference with the −10 °C case in Fig. 4(a), and the predicted ATR using Eq. (13) is within 1.0% error of the actual ATR curve.

$$T_{ad} = T_c(t) - T_{ini} + \lambda_1 \sum (T_c(t) - T_{Amb})\Delta t \quad (13)$$

It is noted that in this study, the foam board insulation type had an RSI value of 0.88 m^2K/W per 2.54 cm layer. If an insulation with a larger RSI value is used, the thickness of the insulation can be reduced. Using the current design, with the plywood formwork and polystyrene foam board insulation, the required insulation (R-value) for each ambient condition is shown in Table 2. To accurately predict the ATR, the actual insulation applied is recommended to be close to the suggested R-value in Table 2. The calculated ATR error would increase if more insulation than the required R-value is used and the ATR would be under predicted using Eq. (13). Furthermore, through FEM analysis, it was found that a smaller size cube (such as 0.5 cubic meter) would have too much heat loss to the environment under the current insulation design, and the heat generation at the center of the cube would be disrupted at an early stage. However, the ATR calculated using Eq. (13) would be accurate for a one-meter cube using the current insulation design.

4. Experiments

The applicability of the proposed procedure for the on-site measurement of adiabatic temperature rise was tested in several field situations. Four on-site castings took place in three different district locations, District 4 (D-4), District 5 (D-5), and District 10 (D-10) in the state of West Virginia. Table 3 shows the mix designs of the delivered concrete. However, the water cementitious (w/cm) ratio of each delivered batch was measured to be 0.5, 0.427, 0.493 and 0.496 for D-4 (OPC), D-4 (Slag), D-5, and D-10, respectively, which are higher than the mix design values, using a revised AASHTO T318-15 method [26]. The measured on-site fresh concrete properties are summarized in Table 4. Type I/II (ASTM C150) ordinary Portland cement (OPC), 50% cement replacement using Grade 100 ground granulated blast furnace slag (used in D-4 and D-5) and 30% cement replacement using Class F fly ash (used in D-10) were used in these concrete mixes. Initial concrete temperature of 24, 30, 25 and 27 °C were recorded for the D-4 (OPC), D-4 (Slag), D-5, and D-10 cubes, respectively. Thermal loggers (Intellirock maturity logger), with an accuracy of ±1 °C, were mounted inside the cubes and activated an hour before the concrete was delivered. Another temperature logger was also installed in a shaded area to record the ambient temperature. Each cube was covered with insulation and plastic sheets after leveling the top surface. The measured temperature histories of the cubes are shown in Fig. 5, showing the center and side center (5-cm from the formwork), and the bottom center (5-cm from the wooden pallet) together with their respective on-site ambient temperatures. The largest peak temperature differences were 1 °C (center versus side) for D-4 (OPC) and 3 °C, 2 °C and 2 °C (center versus bottom) for D-4 (Slag), D-5, and D-10, respectively.

Using the cementitious materials collected on-site during each district casting, the heat generation of each mix was measured with isothermal calorimetry in the laboratory. The isothermal calorimetry, TAM Air micro-calorimeter (8 channels), was used with a 23 °C constant curing temperature. A total of 20-gram cementitious materials was mixed with water for each isothermal test. Water was used as the reference material in the calorimetry.

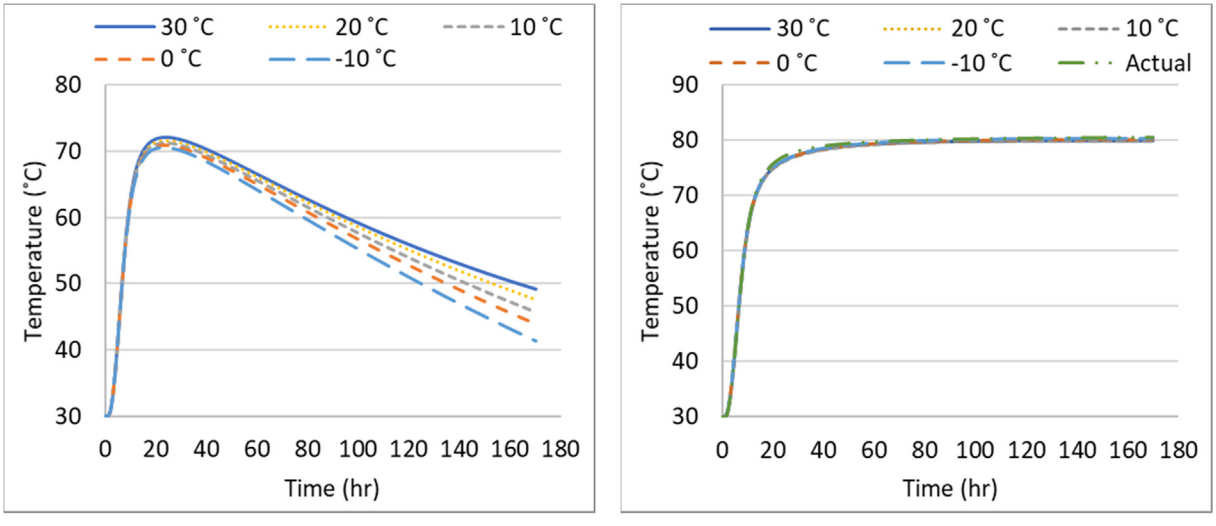

Fig. 4. (a) Center temperatures and (b) Calculated ATRs versus the actual ATR.

Table 3
Mix design of on-site testing.

Material	D-4 (OPC)	D-4 (Slag)	D-5	D-10
Cement (**kg**/**m**^{3})	334.6	150.6	150.6	211.2
Slag (**kg**/**m**^{3})	–	150.6	150.6	–
Fly Ash (**kg**/**m**^{3})	–	–	–	90.17
Water (**kg**/**m**^{3})	163.95	120.55	127.55	120.43
Limestone Aggregate (**kg**/**m**^{3})	969.11	1056.03	1066.11	1056.03
Fine Aggregate (**kg**/**m**^{3})	843.63	864.4	832.36	850.75
Air Entraining (ml/100 kg)	39.15	32.6	81.6	12.4
Retarder, (ml/100 kg)	–	130.5	84.8	228.4
Water Reducer, (ml/100 kg)	–	261	391.5	522
Super Plasticizer, (ml/100 kg)	–	208.8	913.6	287.1

Table 4
Measured on-site fresh concrete properties.

Properties	D-4 (OPC)	D-4 (Slag)	D-5	D-10
Initial Temperature (°C)	24	30	25	27
Slump (cm)	14.6	19.7	17.2	16.5
Air (%)	6.4	8.5	7.8	3.6
Unit density (**kg**/**m**^{3})	2314.64	2350.23	2348.16	2357.63
Measured w/cm ratio	0.5	0.427	0.493	0.496

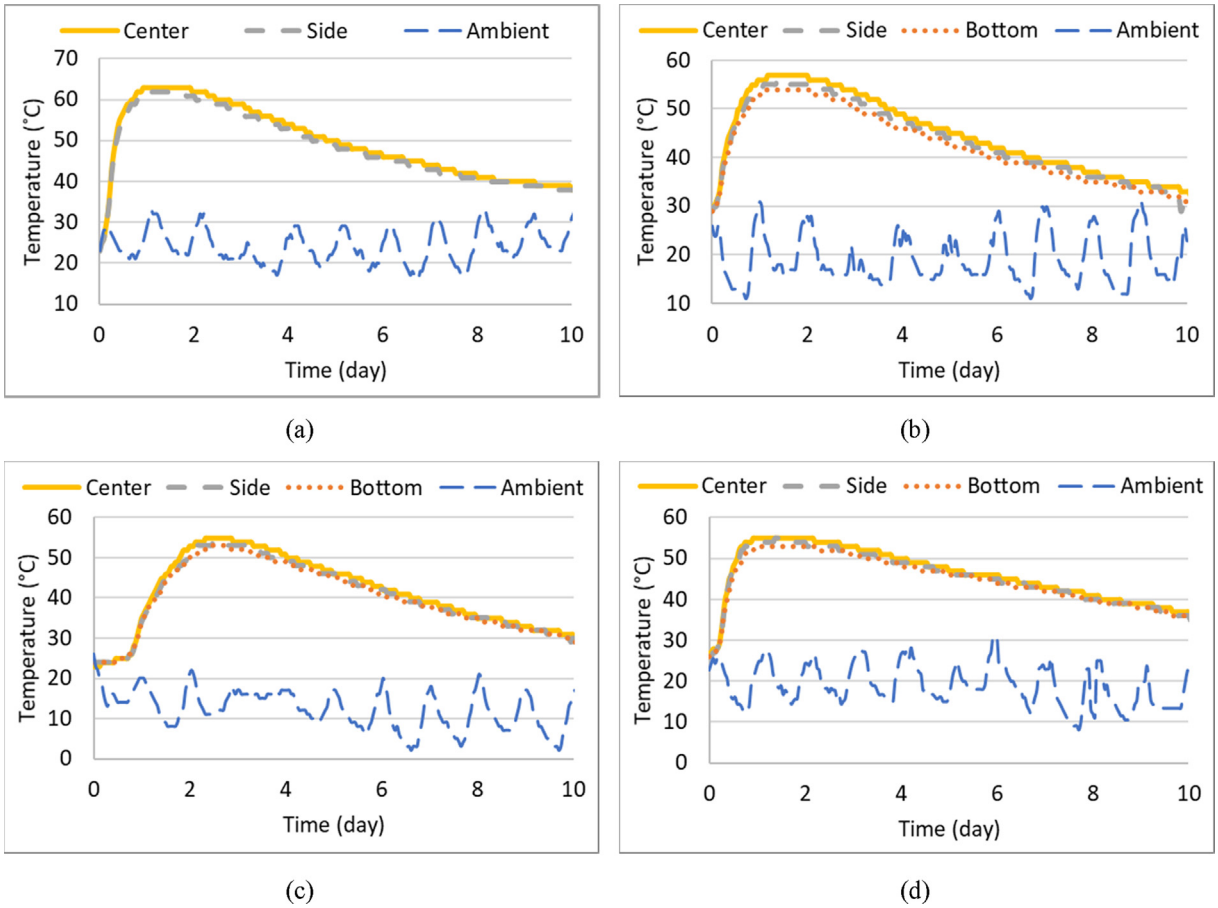

Fig. 5. Measured temperature time histories of 1-m cube test at different site (a) D-4 (OPC) (b) D-4 (Slag) (c) D-5 (d) D-10.

Besides isothermal tests, the adiabatic temperature rise of concrete from each mix design was also tested using an adiabatic calorimeter developed from a previous study [10]. The heat loss was minimized by controlling the surrounding water temperature and matching its temperature with the concrete sample. The sample holder had a layer of polystyrene foam. The accuracy of the temperature measurements was between 0.1 and 0.5 °C using RTD sensors. Chemical compositions of the cementitious materials are

Table 5
Chemical compositions of cementitious materials used.

Chemical Properties	LOI (%)	CaO (%)	SiO_2 (%)	Al_2O_3 (%)	Fe_2O_3 (%)	MgO (%)	SO_3 (%)	Na_2O (%)	K_2O (%)
Cement (D-4)	2.93	63.41	19.91	5.17	3.48	2.55	3.25	0.08	0.84
Cement (D-5)	2.74	63.95	19.61	5.42	4.06	1.19	3.08	0.04	0.66
Cement (D-10)	2.65	63.39	20.19	5.12	3.48	2.17	2.67	0.087	0.83
Fly ash (D-10)	1.5	6.69	43.46	21.06	17.39	0.87	1.68	1.77	1.84
Reference Slag	–	47.48	28.89	8.27	1.93	8.34	0.73	–	–

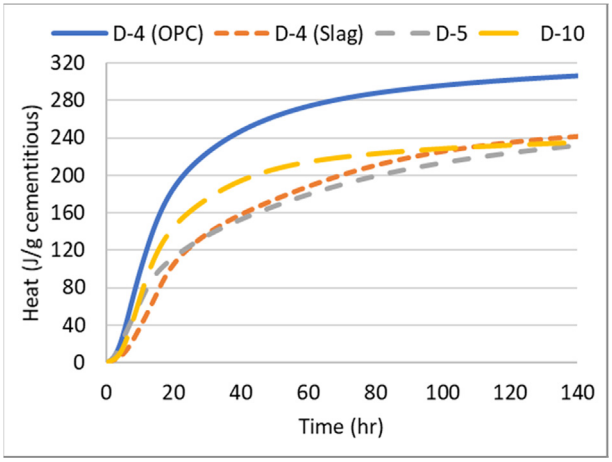

Fig. 6. Measured heat from isothermal calorimetry test of the cementitious materials.

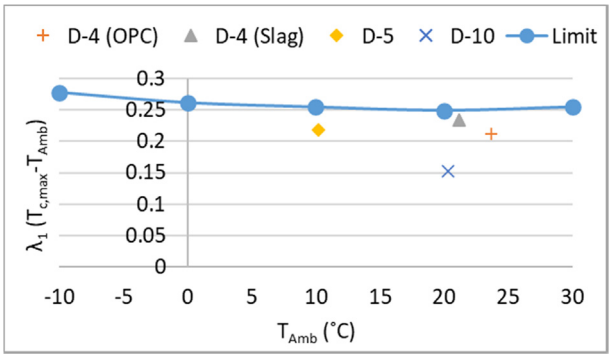

Fig. 7. Cube's heat loss characteristic at different ambient temperature.

shown in Table 5. The isothermal calorimetry measurements are shown in Fig. 6.

5. Results & comparisons

The slope of the best fit line of the measured center temperature between 140 and 200 h was used as $\partial T_c/\partial t$ in Eq. (7) to obtain the average heat loss characteristic coefficient,λ_1, and the average heat loss obtained using the average ambient temperatures (between 140 and 200 h) of the district cubes are shown in Table 6. The value of $\lambda_1(T_{c,max} - T_{Amb})$ for each cube was calculated and plotted versus the Table 2 limitations in Fig. 7. Fig. 7 indicates that the cubes had less heat loss than the upper bound values so the ATR can be obtained accurately. The ATR curves can be calculated using Eq. (13). The calculated ATR curves using the heat loss compensation from each cube center temperature measurement were plotted in Fig. 8. The calculated ATR curves were also plotted in comparison with the measurements from the adiabatic calorimetry and the isothermal calorimetry, and they are plotted in equivalent time as shown in Fig. 9; the results show that the calculated ATR curves agree reasonably with the measured curves. The normalized heat of hydration (J/g binder) measured by the isothermal calorimetry was divided by the density and the specific heat of concrete based on mix design proportions. The densities were 2314.64, 2350.23, 2348.16, and 2357.63 kg/m^3 based on the measured on-site w/cm ratios of D-4 (OPC), D-4 (Slag), D-5 and D-10 delivered batch, respectively. The specific heat was calculated based on Eq. (8). The activation energies for D-4 (OPC) and D-4 (Slag) were measured by fitting the isothermal heat measurements at three different curing temperatures (23 °C, 33 °C, and 43 °C) in equivalent time using Arrhenius Law, Eq. (11), and the results are shown in Table 7. The activation energies of D-5 and D-10 mixes were calculated using Eq. (14) developed by Poole [27]. In Eq. (14), P_{C_3A}, P_{C_4AF}, P_{SO_3}, $P_{Na_2O_{eq}}$, *Blaine*, P_{cem}, P_{FA}, P_{SLAG}, P_{SF}, P_{FA-CaO}, *WRRET* and *ACCL* are the mass proportions of C_3A, C_4AF, SO_3, $(0.658K_2O + Na_2O)$ in Portland cement, Blaine fineness (m^2/kg), the mass proportion of Portland cement, fly ash, slag and silica fume in total cementitious materials and mass proportion of CaO in fly ash, the mass proportion of ASTM Type B&D water reducer/retarder and ASTM Type C calcium-nitrate-based accelerator per gram of cementitious materials, respectively. In the calculation of activation energies of D-5 and D-10 mixes, *WRRET* was assumed to be zero because the retarder and water reducer were not compatible with ASTM Type B&D.

$$E_a = 41,230 + 1,416,000\left[(P_{C_3A} + P_{C_4AF})P_{cem}P_{SO_3}P_{cem}\right] - 347,000P_{Na_2O_{eq}} - 19.8Blaine + 29,600P_{FA}P_{FA-CaO} + 16,200P_{SLAG} - 51,600P_{SF} - 3,090,000WRRET - 345,000ACCL \quad (14)$$

Table 6
Calculated heat loss characteristic coefficient for each cube.

Cube	$T_{c,max}$(°C)	T_{Amb}(°C)	$\lambda_1\left(hr.^{-1}\right)$	$\lambda_1(T_{c,max} - T_{Amb})$
D-4 (OPC)	63	23.7	0.00538	0.2116
D-4 (Slag)	57	21.1	0.00656	0.2355
D-5	55	10.2	0.00488	0.2186
D-10	55	20.3	0.00438	0.1520

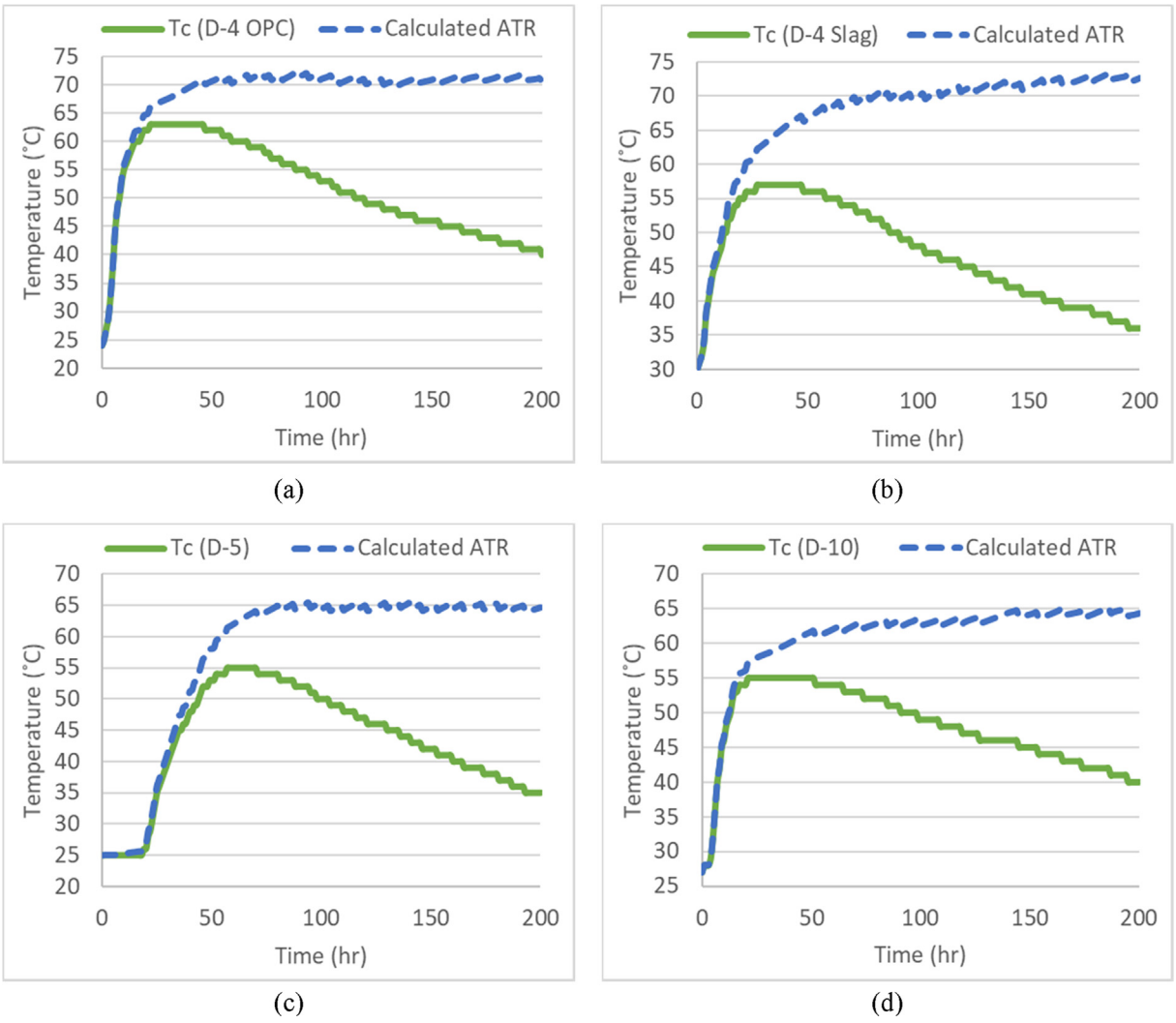

Fig. 8. Calculated ATRs versus the cube's center temperature (a) D-4 (OPC) (b) D-4 (Slag) (c) D-5 and (d) D-10.

It should be noted in Fig. 9(c) that the D-5 ATR based on the isothermal calorimetry was shifted to the beginning of the ATR calorimetry and the heat compensated ATR since the isothermal calorimetry samples were not mixed with chemical admixtures but the D-5 mix had an excessive amount of superplasticizer as seen in Table 3 which delayed the heat of hydration.

The degree of hydration (α) in Eq. (8) was calculated based on the heat release, using Eq. (10), divided by the ultimate heat of hydration, H_u for each concrete mix. The ultimate heat of hydration of Portland cement, H_{cem}, was calculated using Eq. (15) based on the chemical properties of the cement (shown in Table 5), and the ultimate heat of hydration, H_u was calculated using Eq. (16) based on the proportions of cement, slag, and fly ash in the mix design [12]. The ultimate degree of hydration, α_u, was calculated using Eq. (17) based on the w/cm ratio and the proportions of the slag and fly ash [12]. These calculated values are shown in Table 7.

$$H_{cem} = 500P_{C_3S} + 260P_{C_2S} + 866P_{C_3A} + 420P_{C_4AF} + 624P_{SO_3} + 1186P_{freeCaO} + 850P_{MgO} \quad (15)$$

$$H_u = H_{cem}P_{cem} + H_{SL}P_{SL} + 1800P_{FA-CaO}P_{FA} \quad (16)$$

$$\alpha_u = \frac{1.031(w/cm)}{0.194 + w/cm} + 0.50P_{FA} + 0.30P_{SL} \quad (17)$$

where P_{C_3S}, P_{C_2S}, P_{C_3A}, P_{C_4AF}, P_{SO_3}, $P_{freeCaO}$ and P_{MgO} are the mass proportions of Portland cement chemical compounds, SO_3, free CaO (assumed to be 1%) and MgO in Portland cement, respectively. P_{cem}, P_{SL}, P_{FA} are the mass fractions of cement, slag and fly ash in total cementitious materials and P_{FA-CaO} is the mass proportions of CaO in the fly ash. In Eq. (16), H_{SL} was assumed to be 461 (J/g) based on the slag reported in Maekawa et al. [28] with the major chemical compositions of CaO = 43.3% and SiO_2 = 31.3%; this H_{SL} value is assumed for the reference slag used in this study since it has a similar major chemical composition (as shown in Table 5) as the slag in Maekawa et al. [28]. The H_{SL} for the slag used in D-4 and D-5 were obtained based on the isothermal (23 °C) heat measurement of slag in 25% hydrated limewater as a source of alkali. The heat curves generated by the D-4 and D-5 slag were compared to the heat curve from the reference slag in Fig. 10(a). The ultimate heat of the slag assumed by Maekawa et al. (461 J/g) was reduced following the heat ratio between the D-4 and D-5 slag over the reference slag as shown in Fig. 10(b). Based on this observation, the heat from D-4 and D-5 slag approached a constant value of about 70% and 50% of the reference slag, respectively. Therefore, the ultimate heat of the slag, H_{SL} for D-4 and D-5 was assumed to be 322.7 and 230.5 J/g, respectively. The hydration parameters of those four mixes were calculated, Table 7.

Using Eq. (6) and the hydration parameters, the center temperature can be derived and expressed as Eq. (18). Through Eq. (18), τ and β were obtained using the solver function in an Excel program

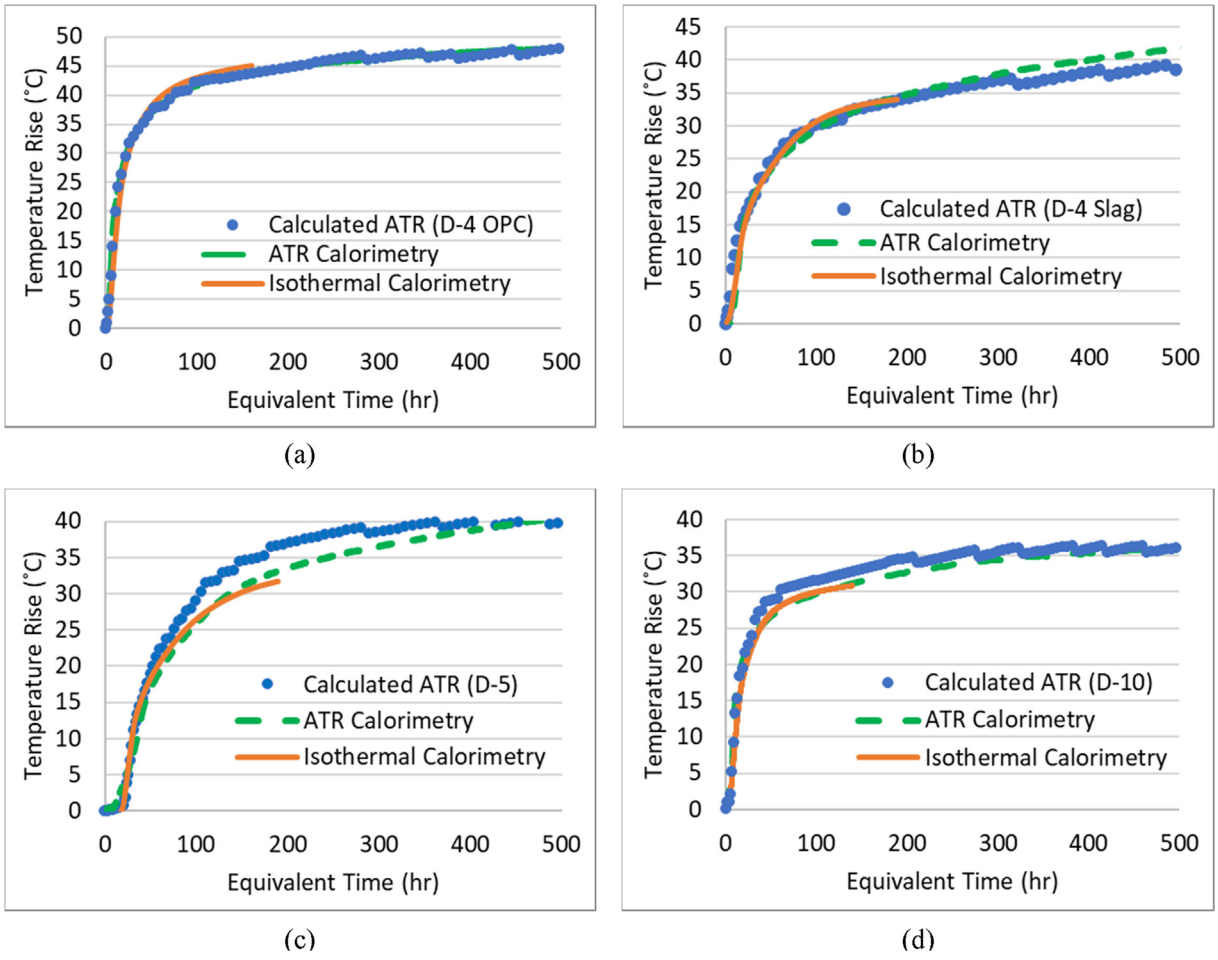

Fig. 9. Adiabatic temperature rise comparison (a) D-4 (OPC) (b) D-4 (Slag) (c) D-5 and (d) D-10.

Table 7
Hydration parameters.

Concrete	τ	β	H_{cem} (J/kg)	H_u (J/kg)	α_u	E_a (J/mol)	W_{cem} (kg/m^3)	W_s (kg/m^3)	W_a (kg/m^3)	W_w (kg/m^3)
D-4 (OPC)	9.60	0.719	492,571	492,571	0.743	37,347	334.6	843.63	969.11	167.3
D-4 (Slag)	22.34	0.537	492,571	407,635	0.859	43,153	301.2	864.4	1056.03	128.6
D-5	19.28	0.913	488,041	359,270	0.889	42,066	301.2	832.36	1066.11	148.49
D-10	13.74	0.588	483,560	374,618	0.891	35,052	301.3	850.75	1056.03	149.48

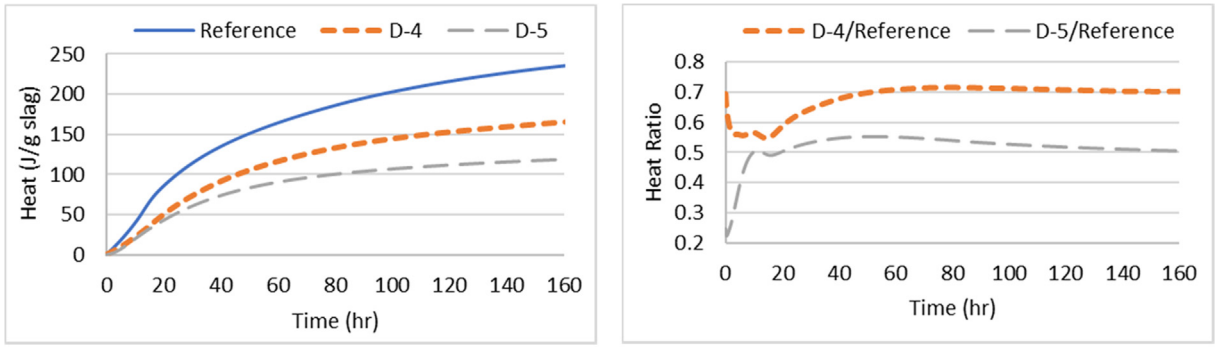

Fig. 10. Comparison of slag materials (a) Heat of hydration (b) Heat Ratios.

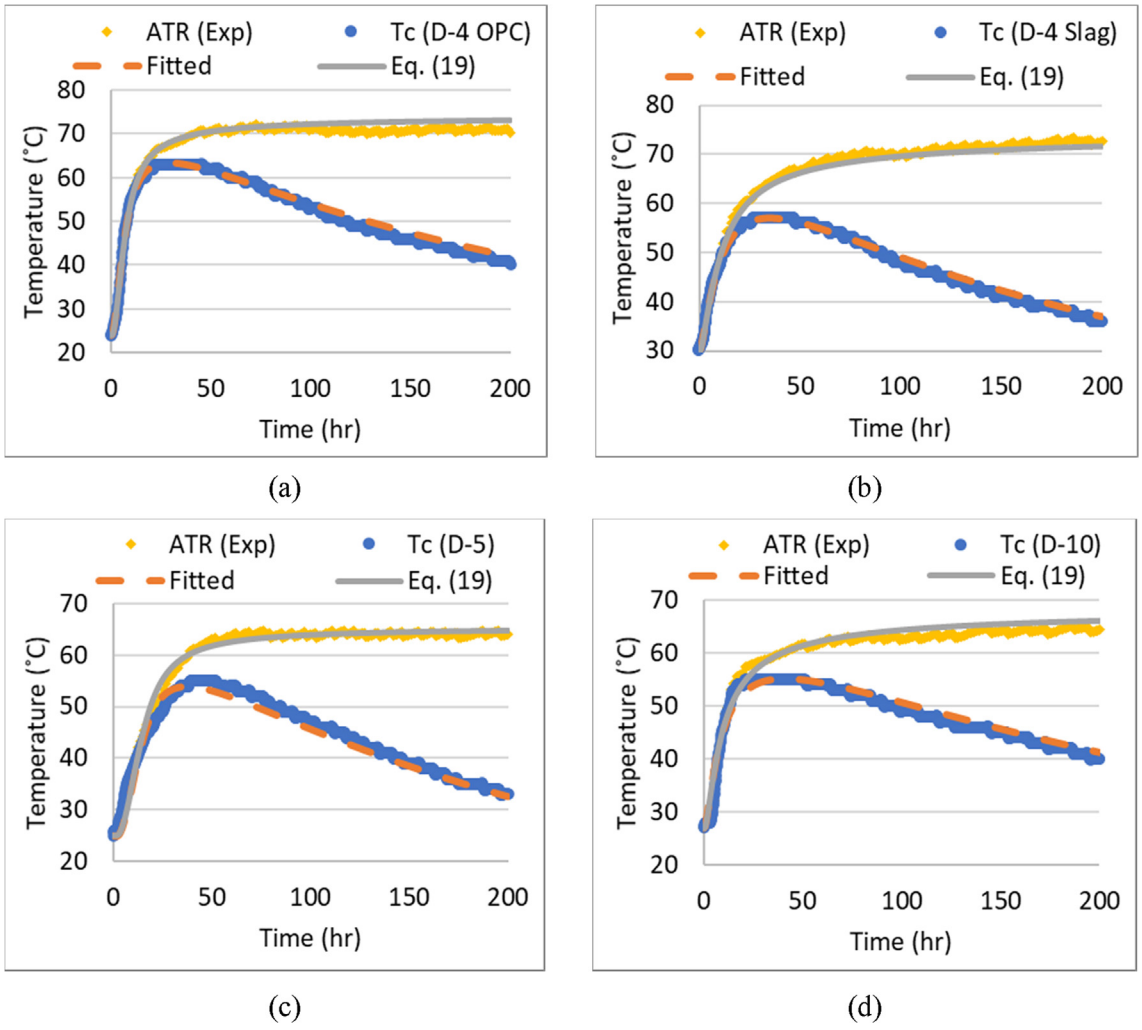

Fig. 11. Comparisons of adiabatic temperature rises (a) D-4 (OPC) (b) D-4 (50% Slag) (c) D-5 (50% Slag) and (d) D-10 (30% Fly Ash).

with an error squares analysis. The summation of errors between the measured center temperature, $T_c(t)$ and Eq. (18) was minimized using the solver function to find the best fit hydration parameters, τ and β for each concrete mix. Eq. (18) was evaluated using a step-by-step numerical integration. A 0.2-hour time step was found to be enough for convergence. The fitted $T_c(t)$ calculated using Eq. (18) for the four concrete mixes compared with the center temperature data from the field tests are shown in Fig. 11. The values of hydration parameters obtained for the four concrete mixes are summarized in Table 7.

$$T_c(t) = \exp(-\lambda_1 t)\left\{\int_0^t \exp(\lambda_1 t)\left[\frac{H_u W_{cem}\alpha_u}{\rho C_p} exp\left(-\left[\frac{\tau}{t_e}\right]^{\beta}\right)\left[\frac{\tau}{t_e}\right]^{\beta} \times \frac{\beta}{t_e}\exp\left(-\frac{E_a}{R^*}\left(\frac{1}{T_{ad}(t)+273}-\frac{1}{23+273}\right)\right)+\lambda_1 T_{Amb}\right]dt + T_{ini}\right\} \quad (18)$$

Using Eq. (10) and Eq. (12), Eq. (19) can be obtained to calculate the ATR using the hydration parameters shown in Table 7.

$$T_{ad}(t) = \left(\frac{H(t)}{\rho C_p(\alpha_r, T(t))}\right),\ H(t) = \int_0^t q(t)dt$$

$$T_{ad}(t) = \left(\frac{W_{cem}H_u\alpha_u}{\rho C_p(\alpha_r, T(t))}\right)\int_0^t \exp\left(-\left[\frac{\tau}{t_e}\right]^{\beta}\right)\left[\frac{\tau}{t_e}\right]^{\beta} \times \frac{\beta}{t_e}\exp\left(-\frac{E_a}{R^*}\left(\frac{1}{T_{ad}(t)+273}-\frac{1}{23+273}\right)\right)dt \quad (19)$$

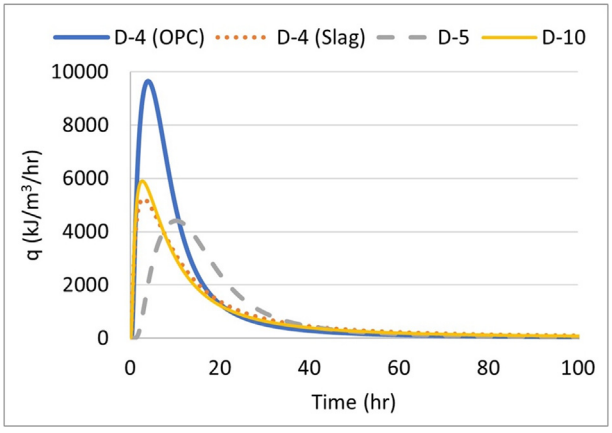

Fig. 12. Comparison of heat generation function q(t) from four mass concrete mixes: D-4 (OPC), D-4 (50% Slag), D-5 (50% Slag) and D-10 (30% Fly Ash).

As shown in Fig. 11, the ATRs calculated based on heat loss compensation using Eq. (13) denoted ATR (Exp), and the ATRs obtained using Eq. (19) are plotted together, and the results show that the experimental curves can be accurately reproduced by the heat of hydration parameters. The heat generation function, $q(t)$ was plotted in Fig. 12 to show the comparison of the heat of hydration for

those four different concrete mixes. As shown in both Fig. 11 and Fig. 12, using 50% slag (in D-4 and D-5) or 30% fly ash (in D-10) replacements of Portland cement greatly reduced the heat of hydration of the concrete. The result of this study shows that for a given mass concrete mix, the heat of hydration can be accurately obtained using the proposed method based on the center temperature measurement of a one-meter cube with adequate insulation.

6. Conclusions

A one-meter cube was developed as an on-site semi-adiabatic calorimeter. A practical method was proposed to simplify the calculation of the adiabatic temperature rise using the measured temperature at the center of the cube. A minimum amount of insulation was needed to satisfy this condition for any ambient temperature so that the calculated ATR had enough accuracy. Based on the minimum insulation requirements, an equation was developed to calculate the cube's center temperature using the heat loss characteristic coefficient and the heat of hydration parameters. The setup was analyzed using the finite element method, and a table was provided for the required insulation in different ambient temperatures ranging from −10 to 30 °C. The results show that the predicted ATR error was less than 1%. The applicability of the proposed procedure for the on-site measurement of the heat of hydration was tested in four different field tests. The calculated ATR from the temperature–time histories of the on-site 1-m cube using the heat loss compensation method compared well with the ATR measured with the laboratory adiabatic and isothermal calorimetry. A set of the heat of hydration parameters was provided based on the ATR calculated from the 1-m cube for each delivered concrete, containing 50% slag or 30% fly ash replacement. The results show that the proposed on-site measurements of the heat of hydration using a 1-m cube located beside the real structure can be a useful, accurate, and practical technique.

CRediT authorship contribution statement

Hung-Liang (Roger) Chen: Conceptualization, Methodology, Software, Writing - review & editing, Supervision, Resources. **Seyednavid Mardmomen:** Methodology, Investigation, Validation, Formal analysis, Software, Data curation, Writing - original draft, Visualization. **Guadalupe Leon:** Investigation, Validation, Software, Writing - review & editing.

Declaration of Competing Interest

The authors declare that they have no known competing financial interests or personal relationships that could have appeared to influence the work reported in this paper.

Acknowledgments

The authors acknowledge the support provided by the West Virginia Department of Transportation Division of Highways and FHWA for the research project WVDOH RP#312. Special thanks are extended to our project monitors, Mike Mance, Ryan Arnold and Donald Williams of WVDOH as well as the District (4, 5 and 10) engineers of WVDOH. The authors also appreciate the assistance from Yun Lin, Alper Yikici, Zhanxiao Ma and WVDOH concrete technicians.

References

[1] G. De Schutter, L. Taerwe, General hydration model for portland cement and blast furnace slag cement, Cem. Concr. Res. 25 (3) (1995) 593–604, https://doi.org/10.1016/0008-8846(95)00048-H.
[2] M. Broda, E. Wirquin, B. Duthoit, Conception of an isothermal calorimeter for concrete— determination of the apparent activation energy, Mat. Struct. 35 (7) (2002) 389–394, https://doi.org/10.1007/BF02483141.
[3] I. Pane, W. Hansen, Investigation of blended cement hydration by isothermal calorimetry and thermal analysis, Cem. Concr. Res. 35 (6) (2005) 1155–1164, https://doi.org/10.1016/j.cemconres.2004.10.027.
[4] E. Gruyaert, N. Robeyst, N. De Belie, Study of the hydration of Portland cement blended with blast-furnace slag by calorimetry and thermogravimetry, J. Therm. Anal. Calorim. 102 (3) (2010) 941–951, https://doi.org/10.1007/s10973-010-0841-6.
[5] J.L. Poole, K.A. Riding, M.C.G. Juenger, K.J. Folliard, A.K. Schindler, Effect of chemical admixtures on apparent activation energy of cementitious systems, J. Mater. Civ. Eng. 23 (12) (2011) 1654–1661, https://doi.org/10.1061/(ASCE)MT.1943-5533.0000345.
[6] X. Pang, W. Cuello Jimenez, B.J. Iverson, Hydration kinetics modeling of the effect of curing temperature and pressure on the heat evolution of oil well cement, Cem. Concr. Res. 54 (2013) 69–76, https://doi.org/10.1016/j.cemconres.2013.08.014.
[7] X. Pang, C. Meyer, R. Darbe, G.p. Funkhouser, Modeling the effect of curing temperature and pressure on cement hydration kinetics, ACI Mater. J., 110 (2) (2013), doi: 10.14359/51685528..
[8] C.T. Tam, Y.H. Loo, K.F. Choong, Adiabatic Temperature Rise in Concrete With and Without GGBFS, ACI SP-149, Oct. 1994, pp. 649–664, doi: 10.14359/4116..
[9] D.R. Petersen, R.E. Link, G.J. Gibbon, Y. Ballim, GRH Grieve, A low-cost, computer-controlled adiabatic calorimeter for determining the heat of hydration of concrete, J. Test. Eval. 25 (2) (1997) 261, https://doi.org/10.1520/JTE11488J.
[10] Y. Lin, H.-L. Chen, Thermal analysis and adiabatic calorimetry for early-age concrete members, J. Therm. Anal. Calorim. 122 (2) (2015) 937–945, https://doi.org/10.1007/s10973-015-4843-2.
[11] Y. Zhang, W. Sun, S. Liu, Study on the hydration heat of binder paste in high-performance concrete, Cem. Concr. Res. 32 (9) (2002) 1483–1488, https://doi.org/10.1016/S0008-8846(02)00810-4.
[12] A.K. Schindler, K.J. Folliard, Heat of hydration models for cementitious materials, ACI Mater. J., 102 (1) (2005), doi: 10.14359/14246..
[13] J.L.P. Kyle, A. Riding, A.K. Schindler, M.C.G. Juenger, K.J. Folliard, Evaluation of temperature prediction methods for mass concrete members, ACI Mater. J. 103 (5) (2006) Sep, https://doi.org/10.14359/18158.
[14] P.L. Ng, I.Y.T. Ng, A.K.H. Kwan, Heat loss compensation in semi-adiabatic curing test of concrete, ACI Mater. J., 105 (1) (2008), doi: 10.14359/19207..
[15] P.L. Ng, A.K.H. Kwan, Semi-adiabatic curing test with heat loss compensation for evaluation of adiabatic temperature rise of concrete, HKIE Trans. 19 (4) (2012) 11–19, https://doi.org/10.1080/1023697X.2012.10669000.
[16] A. Eddhahak, S. Drissi, J. Colin, S. Caré, J. Neji, Effect of phase change materials on the hydration reaction and kinetic of PCM-mortars, J. Therm. Anal. Calorim. 117 (2) (2014) 537–545, https://doi.org/10.1007/s10973-014-3844-x.
[17] B. Klemczak, M. Batog, Heat of hydration of low-clinker cements: Part I. Semi-adiabatic and isothermal tests at different temperature, J. Therm. Anal. Calorim. 123 (2) (2016) 1351–1360, https://doi.org/10.1007/s10973-015-4782-y.
[18] TC Members, TCE1: Adiabatic and semi-adiabatic calorimetry to determine the temperature increase in concrete due to hydration heat of the cement, Rilem, Oct. 01, 1997..
[19] M. Tia, C. Ferraro, A. Lawrence, S. Smith, E. Ochiai, Development of design parameters for mass concrete using finite element analysis, FDOT (2010).
[20] T.A. Do, Finite Element Modeling of Behavior of Mass Concrete Placed on Soil, Doctorate (Ph.D.), University of Florida, Gainesville, Florida, 2013..
[21] T. Yikici, H.L. Chen, Numerical prediction model for temperature development in mass concrete structures, Transp. Res. Rec. 2508 (2015), https://doi.org/10.3141/2508.
[22] K. Van Breugel, Artificial cooling of hardening concrete, Delft University of Technology, 1980.
[23] S. Krishnaiah, D.N. Singh, Determination of thermal properties of some supplementary cementing materials used in cement and concrete, Constr. Build. Mater. 20 (3) (2006) 193–198, https://doi.org/10.1016/j.conbuildmat.2004.10.001.
[24] US Army Corps of Engineers, CRD-C36-73 Method of Test for Thermal Diffusivity of Concrete, CRD-C36-73, 1973..
[25] T.A. Yikici, H.-L. Chen, Use of maturity method to estimate compressive strength of mass concrete, Constr. Build. Mater. 95 (2015) 802–812, https://doi.org/10.1016/j.conbuildmat.2015.07.026.
[26] S. Mardmomen, H.-L. Chen, G. Leon, Revised method for rapid determination of on-site water–cement ratio using microwave oven, Transp. Res. Rec. 2673 (8) (2019) 1–10, https://doi.org/10.1177/0361198119849408.
[27] J.L. Poole, Modeling Temperature Sensitivity and Heat Evolution of Concrete, The University of Texas at Austin, Texas, 2007.
[28] K. Maekawa, T. Ishida, T. Kishi, Multi-Scale Modeling of Structural Concrete, first ed., CRC Press, London; New York, 2009.